RESEARCH ARTICLE

Aberrant functional brain network dynamics in patients with functional constipation

Tao Yin[1,2] 🟢 | Zhaoxuan He[1,2,3] | Peihong Ma[1,2] | Ruirui Sun[1,2] | Kunnan Xie[1] |
Tianyu Liu[4] | Li Chen[1,2] | Jingwen Chen[1] | Likai Hou[5] | Yuke Teng[1,2] |
Yuyi Guo[1] | Zilei Tian[1,2] | Jing Xiong[1] | Fumin Wang[1] | Shenghong Li[6] |
Sha Yang[1,2,3] | Fang Zeng[1,2]

[1]Acupuncture and Tuina School/The 3rd Teaching Hospital, Chengdu University of Traditional Chinese Medicine, Chengdu, Sichuan, China

[2]Acupuncture and Brain Science Research Center, Chengdu University of Traditional Chinese Medicine, Chengdu, Sichuan, China

[3]Key Laboratory of Sichuan Province for Acupuncture and Chronobiology, Chengdu, Sichuan, China

[4]School of Sport, Chengdu University of Traditional Chinese Medicine, Chengdu, Sichuan, China

[5]Sichuan Bayi Rehabilitation Center, Chengdu, Sichuan, China

[6]State Key Laboratory of Southwestern Chinese Medicine Resources/Innovative Institute of Chinese Medicine and Pharmacy, Chengdu University of Traditional Chinese Medicine, Chengdu, Sichuan, China

Correspondence
Fang Zeng and Sha Yang, Acupuncture and Tuina School/The 3rd Teaching Hospital, Chengdu University of Traditional Chinese Medicine, 37 Shierqiao Road, Chengdu, Sichuan 610075, China.
Email: zeng_fang@126.com (F. Z.) and yangsha@cdutcm.edu.cn (S. H.)

Abstract

The aberrant static functional connectivity of brain network has been widely investigated in patients with functional constipation (FCon). However, the dynamics of brain functional connectivity in FCon patients remained unknown. This study aimed to detect the brain dynamics of functional connectivity states and network topological organizations of FCon patients and investigate the correlations of the aberrant brain dynamics with symptom severity. Eighty-three FCon patients and 80 healthy subjects (HS) were included in data analysis. The spatial group independent component analysis, sliding-window approach, k-means clustering, and graph-theoretic analysis were applied to investigate the dynamic temporal properties and coupling patterns of functional connectivity states, as well as the time-variation of network topological organizations in FCon patients. Four reoccurring functional connectivity states were identified in k-means clustering analysis. Compared to HS, FCon patients manifested the lower occurrence rate and mean dwell time in the state with a complex connection between default mode network and cognitive control network, as well as the aberrant anterior insula–cortical coupling patterns in this state, which were significantly correlated with the symptom severity. The graph-theoretic analysis demonstrated that FCon patients had higher sample entropy at the nodal efficiency of anterior insula than HS. The current findings provided dynamic perspectives for

understanding the brain connectome of FCon and laid the foundation for the potential treatment of FCon based on brain connectomics.

KEYWORDS
anterior insula, brain dynamics, functional connectivity, functional constipation, graph theory

1 | INTRODUCTION

Functional constipation (FCon), one of the common functional gastrointestinal diseases (FGIDs, also called disorder of brain–gut interaction) (Drossman & Hasler, 2016), is characterized by infrequent bowel movements and difficulty in defecation (Lacy et al., 2016). It is reported that the global prevalence of FCon ranges from 10.1 to 15.3% (Barberio, Judge, Savarino, & Ford, 2021). Although not a life-threatening disease, FCon seriously influences patients' quality of life and causes high socio-economic burdens (Arco et al., 2021; Nag et al., 2020; Serra et al., 2020). The pathophysiology of FCon has yet been fully understood. Genetics, intestinal hypokinesis, and visceral sensitivity reduction are considered the potential etiologies of FCon (Black, Drossman, Talley, Ruddy, & Ford, 2020; Vriesman, Koppen, Camilleri, Di Lorenzo, & Benninga, 2020). In recent years, the theory of brain–gut interaction was generally recognized (Drossman & Hasler, 2016; Mayer et al., 2019), which provided a new perspective to explain the occurrence and development of FCon from the central nervous system. Evidence from recent neuroimaging studies illustrated that FCon patients had significant structural and functional alterations in brain regions which involved visceral sensorimotor (SM), cognitive control (CC), and emotional regulation (Duan et al., 2021; Hu et al., 2020; Jin et al., 2019; Li et al., 2021; Liu et al., 2021; Peihong et al., 2021; Zhu et al., 2016). Among these altered brain regions in FCon patients, the anterior insula (aINS) was generally regarded as the critical node (Duan et al., 2021; Jin et al., 2019; Liu et al., 2021; Zhu et al., 2016) for its essential role in processing interoceptive signals (Mayer, 2011), modulating visceral activities (Rubio et al., 2015), and regulating emotions and cognitions (Craig, 2009).

Resting-state functional connectivity (rsFC) reflects the time-series correlations of the blood-oxygenation-level-dependent (BOLD) signals between the functionally related brain regions in the absence of any task (Biswal, Yetkin, Haughton, & Hyde, 1995). In the last two decades, rsFC has been accepted as a powerful tool for decoding the spatiotemporal organizations of spontaneous cerebral activity. Using rsFC analysis, researchers have revealed the disrupted static coupling patterns and topological characteristics of the intrinsic brain networks in patients with FCon and other FGIDs (Jin et al., 2019; Liu et al., 2021; Osadchiy et al., 2020; Zeng et al., 2019; Zhu et al., 2016). However, these conventional rsFC analyses were founded on an implicit assumption that functional interactions of the brain remained relatively static over the entire scan (Calhoun, Miller, Pearlson, & Adalı, 2014), and therefore inevitably omitted the important information describing the time-varying properties of signal processing in the human brain. In fact, subjects maintained uncontrolled fluctuations in neural activity throughout the entire resting-state scanning (Chang & Glover, 2010; Li, Duan, Cui, Chen, &

Liao, 2019). The connectivity patterns of brain networks were also varied at different temporal scales (Zhuang et al., 2020). Therefore, quantifying the variations of rsFC metrics over time may aid in capturing the functional dynamics which diluted by conventional approaches and provide greater insight into the fundamental properties of brain networks. The sliding-window-based dynamic functional connectivity (dFC) (Preti, Bolton, & Van De Ville, 2017) provided a promising approach to quantify the time-variation of rsFC metrics and largely improved our knowledge of the functional dynamics of the brain (Calhoun et al., 2014). Recently, a growing number of sliding-window-based dFC studies were performed, and many encouraging results were obtained (Díez-Cirarda et al., 2018; Fiorenzato et al., 2019; Kim et al., 2017; Mäki-Marttunen & Espeseth, 2021). For example, the dFC patterns in the early stages could sensitively characterize the mild cognitive deficits and predict the disease progression of patients with Parkinson's disease (Díez-Cirarda et al., 2018; Kim et al., 2017). These results suggested that more valuable information could be decoded with dynamic analysis models, allowing for more accurate characterization of the brain functional organization of the human being.

As a typical disorder of brain–gut interaction, the alterations of the static brain rsFC pattern in FCon patients have been widely illustrated (Duan et al., 2021; Jin et al., 2019; Li et al., 2021; Liu et al., 2021). However, there was currently no study addressing the dFC patterns of FCon patients. The time-variation of brain co-activation and topological organizations in FCon patients remained largely unknown, which limited our further understandings of the pathophysiology of FCon. Therefore, applying the resting-state functional magnetic resonance imaging (fMRI) data and the sliding-window-based dFC analysis, we performed this study and aimed to compare the (a) dynamic connectivity patterns, which were reflected by the temporal properties and coupling patterns of the dFC states and (b) dynamic network topological organizations, which were measured with the sample entropy (SampEn) of graph-theoretic metrics of the functional brain networks between FCon patients and healthy subjects (HS). We hypothesized that FCon patients manifested disrupted dynamic connectivity patterns and atypical dynamic topological organizations in the intrinsic functional brain networks. These alterations would significantly associate with the constipation symptoms.

2 | MATERIALS AND METHODS

2.1 | Participants

This study enrolled 90 FCon patients and 90 HS. Patients were recruited from the Hospital of Chengdu University of Traditional Chinese

Medicine and the campus of Chengdu University of Traditional Chinese Medicine from September 2018 to January 2020. After being diagnosed by two gastroenterologists according to the Rome IV Diagnostic Criteria for FCon (Lacy et al., 2016) and undergoing physical and laboratory examinations (Yin et al., 2019), the potential patients who met the following inclusion criteria were included: (a) were right-handed and aged from 18 to 40 years, (b) did not take any gastrointestinal prokinetic agent or laxative at least 15 days before enrollment, (c) did not participate in any clinical trial in the past 3 months, and (d) signed informed consent. Patients were excluded if they (a) suffered from organic or metabolic diseases; (b) had organic changes in the rectum (such as lumps or rectal stenosis) examined by rectal fingerprints; (c) were afflicted with acute or chronic pain disorders, or severe depression, or anxiety; (d) had a history of head trauma, gastrointestinal surgery, or psychiatric or neurological disorders, (e) were pregnant or lactating, or intended to pregnant in the 6 months, and (f) had any contraindication of MRI scans such as implanted ferromagnetic metal or claustrophobia.

The 90 right-handed HS (aged from 18 to 40 years) were recruited by the advertisement at the campus of Chengdu University of Traditional Chinese Medicine. These volunteers had never been diagnosed with gastrointestinal, neurological, or psychiatric disorders and were evaluated with comprehensive history taking, physical examinations, and laboratory tests to exclude the potential diseases.

2.2 | Trial registration

This study was registered in the Chinese Clinical Trial Registry on June 14, 2018 (Registered number: ChiCTR1800017689) and was conducted following the principles of the Declaration of Helsinki.

2.3 | Symptom measurement

The enrolled patients were required to complete a 2-week stool diary to record the weekly spontaneous bowel movements (SBMs). At the end of the 2-week observation period, the Patient Assessment of Constipation Symptom Questionnaire (PAC-SYM) and the PAC Quality of Life Questionnaire (PAC-QoL) were used to evaluate the severity of constipation symptoms and the influences of constipation symptoms on QoL of FCon patients. In addition, the Zung Self-Rating Anxiety Scale (Zung, 1971) (SAS) and Self-Rating Depression Scale (Zung, 1965) (SDS) were applied to measure the mental state of both the patients and HS.

2.4 | MRI data acquisition

MRI data were acquired with a 3.0 T magnetic resonance scanner with an eight-channel-phased array head coil (GE Discovery 750, Milwaukee, WI) at the MRI research center of the University of Electronic Science and Technology of China. Participants were asked to keep their heads still and awake during the scan, with their eyes closed and ears plugged. Parameters of the high-resolution three-dimensional T1-weighted imaging were as follows: repetition time (TR)/echo time (TE) = 6.008 ms/1.7 ms, slice thickness = 1 mm, slice number = 156, matrix size = 256 × 256, and field of view = 256 × 256 mm^2. The BOLD MRI data were acquired with the echo-planar imaging: TR/TE = 2,000 ms/30 ms, flip angle = 90°, slice number = 31, matrix size = 64 × 64, field of view = 240 × 240 mm^2, slice thickness = 5 mm, total volume = 180.

2.5 | MRI data preprocessing and head motion control

The MRI data preprocessing was performed with SPM12 (http://www.fil.ion.ucl.ac.uk/spm) and DPARSF4.1 (http://rfmri.org/DPARSF) (Yan, Wang, Zuo, & Zang, 2016). First, the beginning 10 timepoints were discarded, allowing for signal stabilization. The remaining images were corrected for slice-timing and head motion. Then the corrected images were normalized to the Montreal Neurologic Institute space and smoothed with a 4 mm Gaussian kernel of full width at half maximum.

As excessive head motion significantly affects the reliability of rsFC analysis (Hutchison et al., 2013; Van Dijk, Sabuncu, & Buckner, 2012), we applied a strict inclusion criteria to minimize the potential bias caused by head motion. Namely, participants were excluded if the mean framewise displacement (FD) (Power, Barnes, Snyder, Schlaggar, & Petersen, 2012) > 0.2 mm, or percentage of the FD exceeded 0.2 mm > 30%, or the maximum displacement > one voxel size. In addition, following the correction strategy recommend by recent studies (Ciric et al., 2017; Kim et al., 2017; Luppi et al., 2019), the six rigid-body motion parameters and signals of white matter and CSF were regressed out using the component-based noise correction method (Behzadi, Restom, Liau, & Liu, 2007) to minimize the influences of head motion on the estimation of the functional connectivity matrices.

2.6 | dFC analysis

The framework of dFC analysis contained four steps (Figure 1). In Step 1, the spatial group independent component analysis (GICA) was performed to decompose the whole-brain resting-state fMRI data into multiple independent components (ICs). Then, the selected ICs were sorted into seven intrinsic connectivity networks (ICNs) based on their spatial maps. In Step 2, the dFC matrices among these ICNs were estimated using the sliding-window approach. In Step 3, the k-means clustering method was applied to cluster the windowed matrices into multiple separate sets to identify the dFC states, followed by comparing the temporal properties and coupling patterns of these states between FCon patients and HS. In Step 4, the SampEn of graph-theoretic metrics across scanning was calculated to assess the disorderliness of network topological organizations in both FCon patients and HS.

Step 1: GICA analysis and ICNs selection

Step 2: dFC Computation

Step 3: State clustering analysis

Step 4: Dynamic graph-theoretic analysis

FIGURE 1 The framework of dFC analysis. AUC, area under the curve; dFC, dynamic functional connectivity; E_{glob}, global efficiency; E_{loc}, local efficiency; E_{nodal}, nodal efficiency; GICA, group independent component analysis; ICNs, intrinsic connectivity networks; ICs, independent components; K_{nodal}, nodal degree; ROI, region-of-interest; SampEn, sample entropy

2.7 | Step 1: GICA

The spatial GICA was performed using the GIFT v3.01 toolbox (https://trendscenter.org/software/gift/). First, we applied the Infomax algorithm (Bell & Sejnowski, 1995) to decompose the resting-state fMRI data of all participants into a set of ICs, and utilized the two-step component selection approach (Allen et al., 2014) to

estimate ICs. Namely, for the subject-wise data reduction, a total of 120 principal components were reserved using the principal component analysis. For the group-level data reduction, the reserved components were concatenated and then were decomposed into 100 ICs. The reliability and stability of the Infomax algorithm were assessed by repeating the ICA process 20 times with ICASSO toolbox in GIFT (Himberg, Hyvärinen, & Esposito, 2004). Only ICs with average

intracluster similarity greater than 0.8 were reserved (Fiorenzato et al., 2019). Subsequently, the subject-specific spatial maps and corresponding time courses of each IC were back-projected from the group spatial maps using the GICA back reconstruction algorithm (Calhoun, Adali, Pearlson, & Pekar, 2001).

After dropping out the components with low intracluster similarity, we identified the ICs following the criteria recommended by Allen et al. (2014): (a) spatial maps of ICs overlapped with the known brain regions, (b) peak coordinates of ICs located in the gray matter, (c) time courses of ICs dominated by low-frequency signals, and (d) time courses of ICs presented with a high dynamic range. Based on the anatomical and presumed functional properties (Allen et al., 2014), the identified ICs were sorted into seven ICNs. Afterward, the time courses of the selected ICs were postprocessed with the following steps to remove the physiological and scanner noises (Allen et al., 2014): (a) detrending linear, quadratic, and cubic trends; (b) despiking the detected outliers with 3dDespike algorithm; (c) filtering with a high-frequency cutoff of 0.15 Hz; and (d) regressing out the six rigid-body motion parameters. After generating the spatial maps and time courses of ICNs for all participants and finishing the postprocessing steps described above, we conducted a one-sample t test for each spatial map to obtain the group-level spatial map for each IC and estimated the static functional connectivity matrix across participants with the pair-wise Pearson's correlations among these ICs.

2.8 | Step 2: Estimation for dFC matrices

The dFC analysis was conducted with the dynamic FNC toolbox in GIFT. The sliding-window approach was applied to estimate the dFC of the identified ICNs across the 170 timepoints. The window length was set to 22 TR (44 s), as it was reported to provide a good compromise between the ability in capturing the dynamic patterns of functional connectivity and the quality of the correlation matrix estimation (Allen et al., 2014; Fiorenzato et al., 2019; Kim et al., 2017). And then, these segmented windows were convolved with Gaussian (sigma = 3 TR) and slid in the step of 1 TR, generating 148 consecutive windows for each subject. To eliminate the unwanted noises introduced by covariance estimation using shorter time series, the regularized inverse covariance matrix was introduced (Smith et al., 2011). Specifically, a penalty on the L1 norm of the precision matrix was imposed in the graphic LASSO framework with 100 iterations to promote sparsity (Friedman, Hastie, & Tibshirani, 2008). Subsequently, all the obtained functional connectivity matrices were transformed to z scores using Fisher's z-transformation.

2.9 | Step 3: State clustering analysis

K-means clustering is an unsupervised machine learning algorithm that aims to divide data into several sets in the absence of labels, allowing the data within each set to be as similar as possible and the sets to be

as different from each other as possible. The brain transient functional connectivity patterns iterate following a specific pattern of turnover even within a short scanning time (6–8 min) (Calhoun et al., 2014), which makes it possible to investigate the reoccurring states of functional connectivity using the clustering method. In this study, we conducted the k-means clustering analysis for all windowed matrices (148 × 163 matrices) to estimate the reoccurring functional connectivity states. The L1 distance function was introduced to assess the within-cluster similarity between each windowed matrix and the cluster centroids. The optimal number of cluster centroids was determined by the elbow criterion, which was defined as the ratio of within-cluster distance to between-cluster distance (Tu et al., 2019). To reduce redundancy between windows and computational burden, before the k-means clustering analysis, windows were subsampled along the time dimension for each participant. Similar to EEG microstate analysis (Pascual-Marqui, Michel, & Lehmann, 1995), those matrices with local maxima in functional connectivity variance were chosen as the subject-specific exemplars (Allen et al., 2014; Tu et al., 2019). The clustering analysis was conducted on these chosen exemplars to obtain the cluster centroids of states. To reduce the bias of the initial random selection of cluster centroids, the k-means algorithm was repeated 100 times on these subsampling windows. With the obtained state centroids as the initialization, all windowed matrices of participants were then categorized into one of these states based on the similarity with cluster centroids. The subject-specific centroids in each state were calculated by computing the median matrices of each participant in that state. The group-specific centroids of FCon patients and HS in each state were calculated by averaging the subject-specific centroids in that state.

To evaluate the temporal properties of these reoccurring functional connectivity states, we calculated three different metrics about state transition: the occurrence rate, the mean dwell time, and the number of transitions. The occurrence rate referred to the proportion of time spent in each state as measured by percentage. The mean dwell time represented the average time that the consecutive windows stayed in each state. The number of transitions was defined as the number of transitions from any state to other states. The differences of these above transiting metrics in each state were examined by the two-sample t test or Mann–Whitney U test between FCon patients and HS. The significance threshold was set to $p < .05$, false discovery rate (FDR) corrected. Additionally, the Pearson's correlation or Spearman's correlation analyses between these transiting metrics and clinical symptoms were conducted to investigate the associations between the altered temporal properties of functional connectivity states and the severity of symptoms in FCon patients.

After comparing the transiting metrics of each state between FCon patients and HS, we further analyzed the coupling patterns of those states with significant between-group differences in temporal properties. Considering the critical role of the aINS in viscerosensory perception and transmission (Mayer, 2011), as well as the disrupted structural and functional connectivity patterns of the aINS in FCon patients (Liu et al., 2021; Nan et al., 2018; Zhu et al., 2016), the IC located at the aINS was selected as the region-of-interest (ROI). The

between-group comparison was performed on these connections with aINS to investigate the alterations of the functional coupling patterns in these differentiating states of FCon patients. The significance threshold was set to $p < .05$, FDR corrected. Moreover, the associations between clinical symptoms and functional coupling patterns of the aINS in FCon patients were investigated with the Pearson's correlation analyses, with the significance threshold setting at $p < .05$, FDR corrected.

2.10 | Step 4: Dynamic graph-theoretic analysis

SampEn measures the disorderliness and instability of the time-based physiological signals (Nezafati, Temmar, & Keilholz, 2020; Richman & Moorman, 2000). Previous studies on the SampEn of fMRI data have indicated that healthy and diseased individuals exhibited significantly different disorderliness in BOLD signals (Easson & McIntosh, 2019; Shafiei et al., 2019; Shan et al., 2018). Inspired by these studies, we introduced SampEn into the dynamic graph-theoretic analysis for the first time, to reflect the differences in the stability of information transmission of brain networks between FCon patients and HS.

The dynamic graph-theoretic analysis was performed based on the 163×148 matrices generated in Step 2. First, the topological metrics of each matrix were computed using graph-theoretic analysis (Rubinov & Sporns, 2010). Then the SampEn (Richman & Moorman, 2000) of these topological metrics in the 148 consecutive windows were calculated to reflect the dynamic topological organizations of the functional brain networks in both FCon patients and HS.

The graph-theoretic analysis was conducted with the GRETNA toolbox (Wang et al., 2015) (http://www. nitrc.org/projects/gretna). The global measures, including global efficiency (E_{glob}) and local efficiency (E_{loc}), as well as the regional nodal measures including nodal efficiency (E_{nodal}) and nodal degree (K_{nodal}) of the ROI (the aINS), were calculated for each matrix. The E_{glob} is a functional integration metric that reflects the ability of parallel information transmission over the network. The E_{loc} is a functional segregation metric that represents the communication speed among the densely interconnected nodes. Similar to the E_{glob}, The E_{nodal} of a given node characterizes the efficiency of parallel information transfer of that node in the network. The K_{nodal} of a given node reflects its information communication ability in the network. The formula and interpretation of the above topologic metrics were introduced at Rubinov's (Rubinov & Sporns, 2010) and Wang's (Wang et al., 2011) studies. In order to keep the networks with the same number of edges or wiring cost, the sparsity thresholds were set to a specific range. As recommended by previous studies (Tu et al., 2019; Yu et al., 2017), we utilized the sparsity threshold ranging from 0.1 to 0.35 with 0.05 increment to sparsity all matrices. Thereafter, the undirected and unweighted adjacency matrix for each participant at each window was generated by setting edges as 1 or 0. Specifically, edges were designated as 1 if the absolute values of edges between nodes i and j were greater than the threshold, otherwise, edges were designated as 0. The selected topologic metrics

were evaluated at each sparsity threshold, and the area under the curve (AUC) of these metrics was calculated within the defined threshold range to avoid the bias caused by the specific selection of thresholds (Liu et al., 2021). The time series of AUCs in the 148 consecutive windows were applied to calculate the SampEn of these four topologic metrics.

Referencing the equation and code provided in Luppi et al.'s (2019) article (https://uk.mathworks.com/matlabcentral/fileexchange/35784-sampleentropy), we calculated the SampEn of each topologic metric in the 148 consecutive windows for both FCon patients and HS. The parameters were set following the recommended parameters in this code: the embedded dimension $= 2$, the delay time for downsampling $= 1$, and the tolerance $= 0.2 \times SD$ of signals. Thereafter, the two-sample t tests were conducted to compare the differences of the SampEn of the four topologic metrics between FCon patients and HS, with the significance threshold setting to $p < .05$, FDR corrected.

3 | RESULTS

Seven FCon patients and ten HS were excluded due to the excessive head motion. Therefore, 83 FCon patients and 80 HS were included in data analysis. There was no significant difference in mean FD between FCon patients and HS (FCon patients: 0.079 ± 0.026, HS: 0.083 ± 0.030, $p = .398$). The demographic and clinical characteristics of participants are displayed in Table 1. There was no significant difference in age and gender between FCon patients and HS ($p > .05$). Although FCon patients had higher SAS and SDS scores than HS ($p < .05$), neither the SAS nor the SDS scores of FCon patients met the diagnosis of anxiety or depression.

3.1 | Intrinsic connectivity networks

Seventeen ICs were dropped out due to the lower average intracluster similarity (less than 0.8) in ICASSO analysis (Supplementary information 1). The retained 83 ICs were subsequently evaluated following the established ICs selection criteria and 60 ICs were finally reserved. These ICs were consistent with the spatial maps of ICNs derived from previous ICA decomposition (Allen et al., 2014; Tu et al., 2019). According to the anatomical location and function, these 60 ICs were categorized into the following 7 ICNs: the subcortical network (SC: ICs 6, 48, 66, and 73); the auditory network (AUD: ICs 7 and 13); the SM network (ICs 1, 2, 4, 5, 23, 35, 44, 47, 52, and 84); the visual network (VS: ICs 9, 10, 15, 21, 24, 26, 33, 34, 42, 50, 67, 72, and 78); the CC network (ICs 14, 17, 18, 19, 20, 27, 28, 30, 31, 32, 54, 56, 58, 62, 63, 65, 76, 79, 83, and 98); the default mode network (DM: ICs 39, 40, 49, 68, 75, and 81); and the cerebellum network (CB: ICs 11, 25, 51, 70, and 71) (Figure 2a). The subject-averaged static functional connectivity matrix is displayed in Figure 2b. The detailed information and spatial maps of these identified ICs are provided in Supplementary information 2 and 3.

TABLE 1 The demographic and clinical characteristics of FCon patients and HS

	Age (year)	Gender (M/F)	SAS score	SDS score	Duration (months)	Weekly SBMs	PAC-SYM score	PAC-QoL score
FCon (n = 83)	20.24 ± 2.15	6/77	40.87 ± 8.87	44.85 ± 10.43	60.08 ± 31.14	2.58 ± 0.96	16.76 ± 5.66	37.73 ± 14.18
HS (n = 80)	20.84 ± 2.20	8/72	36.38 ± 6.41	37.54 ± 6.94	N/A	N/A	N/A	N/A
p-Value	.081	.585	3.1e-4*	1.0e-6*	N/A	N/A	N/A	N/A

Note: No significant difference was found in age and gender between FCon and HS (p > .05). FCon patients had higher SAS and SDS scores than HS (*p < .05).
Abbreviations: FCon, functional constipation; HS, healthy subjects; M/F, male/female; PAC-QoL, Patient Assessment of Constipation Quality of Life Questionnaire; PAC-SYM, Patient Assessment of Constipation Symptom Questionnaire; SAS, Self-Rating Anxiety Scale; SBMs, spontaneous bowel movements; SDS, Self-Rating Depression Scale.
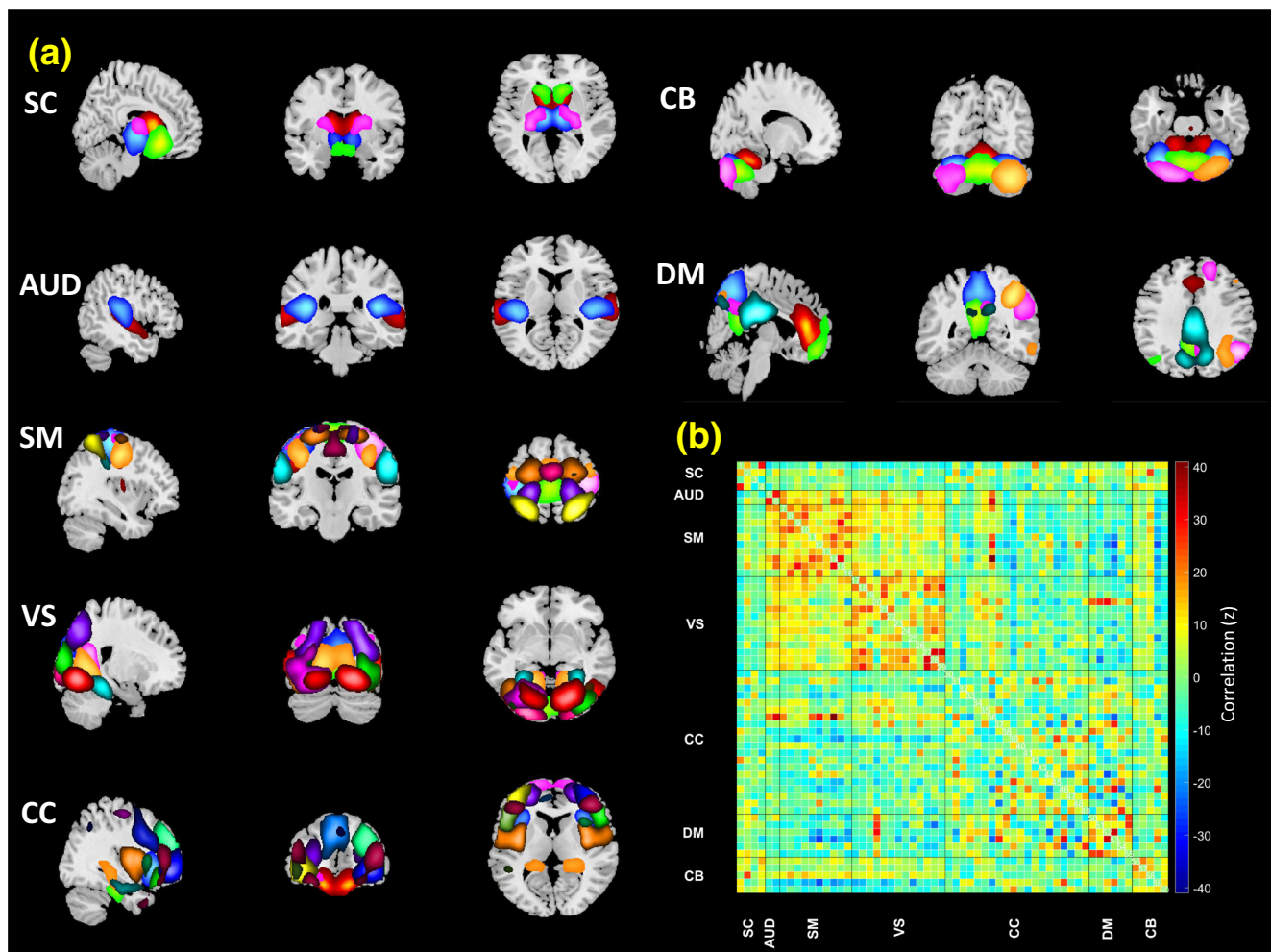

FIGURE 2 ICNs identified at spatial GICA. (a) The spatial maps of these seven ICNs. (b) The subject-averaged static functional connectivity matrix. AUD, auditory network; CB, cerebellum network.; CC, cognitive control network; DM, default mode network; GICA, group independent component analysis; SC, subcortical network; SM, sensorimotor network; VS, visual network

3.2 | State clustering analysis

The cluster centroids of states and their occurrence rate are shown in Figure 3a. The edges with connection strength greater than 0.25 in each centroid are shown in Figure 3b. As illustrated in Figure 3a,b, the coupling patterns were different among these cluster states. States 1, 2, and 4 had the less frequent (22% in State 1, 24% in State 2, and 9% in State 4) but stronger positive connectivities within VS, SM, and

AUD. State 3 showed more frequent (45%) but relatively sparse connections in the whole brain. In addition, State 2 manifested strong positive or negative connectivities between multiple ICs across CC and DM. State 4 manifested strong negative connectivities between VS/SM/AUD and CB/SC. Figure 3c,d displays the group-specific cluster centroids of FCon patients and HS of each state, which had similar connecting characteristics with the cluster centroids obtained across all participants. We performed between-group comparisons of these
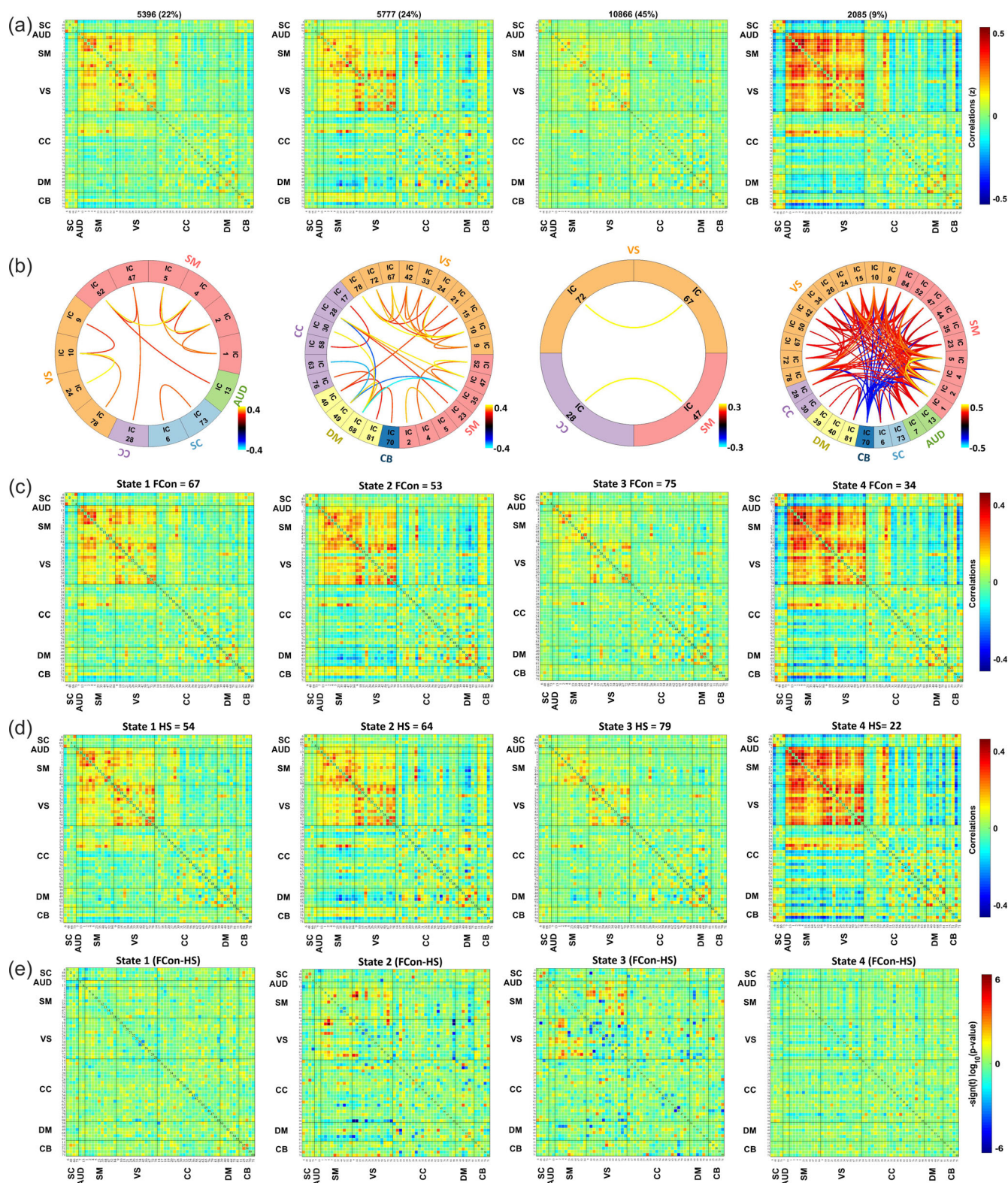
FIGURE 3 Results of the state clustering analysis. (a) The cluster centroid of each state and its corresponding occurrence rate. (b) The connectogram of edges with connection strength greater than 0.25 in each state. The warm-toned lines indicate positive connectivity, and the cold-toned lines indicate negative connectivity. (c,d) The cluster centroids and occurrence of FCon patients and HS in each state, respectively. The occurrence of each state was calculated by summing the numbers of subjects with at least one window belonging to that state. (e) The result of between-group comparisons of the centroids in FCon patients and HS in these states. The red grids and blue grids indicate the edges that the functional connectivity in FCon patients is stronger or weaker than HS, respectively. AUD, auditory network; CB, cerebellum network; CC, cognitive control network; DM, default mode network; FCon, functional constipation; HS, healthy subjects; SC, subcortical network; SM, sensorimotor network; VS, visual network

four cluster centroids in FCon patients and HS, finding the more pronounced between-group differences of connectivity patterns in States 2 and 3 (Figure 3e).

3.3 | Temporal properties of dFC states

Since the temporal properties did not follow a normal distribution, the Mann–Whitney U test was applied here to compare the between-group differences of temporal properties in FCon patients and HS. The results indicated that FCon patients had significantly lower occurrence rate in State 2 than HS (FCon patients: 0.155 ± 0.197, HS: 0.327 ± 0.297, p = 2.3e-5, p_{FDR} < .05) but no significant difference in other states (Figure 4a). Similarly, FCon patients also manifested significantly decreased mean dwell time in State 2 than HS (FCon patients: 9.341 ± 10.880, HS: 19.264 ± 17.990, p = 3.2e-5, p_{FDR} < .05) (Figure 4b). However, no significant difference in number of transitions was detected between FCon patients and HS (FCon patients: 5.566 ± 3.065, HS: 5.600 ± 2.637, p = .799) (Figure 4c). The results of Spearman's correlation analyses demonstrated that both the occurrence rate and the mean dwell time in State 2 positively associated with the weekly SBMs (r = .239,

p = .030, p_{FDR} > .05; r = .237, p = .031, p_{FDR} > .05) (Figure 4d,e), and that the mean dwell time in State 2 positively correlated with the duration (r = .225, p = .041, p_{FDR} > .05) in FCon patients with a uncorrected threshold (Figure 4f).

After regressing the influences of age, gender, mean FD, SAS score, and SDS score, the between-group differences of the occurrence rate and mean dwell time in State 2 were still significant (p = 4.2e-5; p = 2.9e-5). Moreover, after controlling these above covariates, the correlations between the occurrence rate in State 2 and weekly SBMs, as well as between the mean dwell time in State 2 and weekly SBMs were increased significantly (r = .340, p = .002, p_{FDR} < .05; r = .324, p = .004, p_{FDR} < .05) (Supplementary information 4a,b).

Considering the potential influences of the window length on the results of the k-means clustering, we also performed dFC analysis with the window length setting to 20TR (40 s) and 24TR (48 s), respectively. The results indicated that the cluster centroids obtained with different window lengths had similar connectivity patterns. Moreover, the aberrant temporal properties of State 2 of FC patients could also be reproduced when the window length setting to 20TR and 24TR. See Supplementary information 5 for more details of the results.
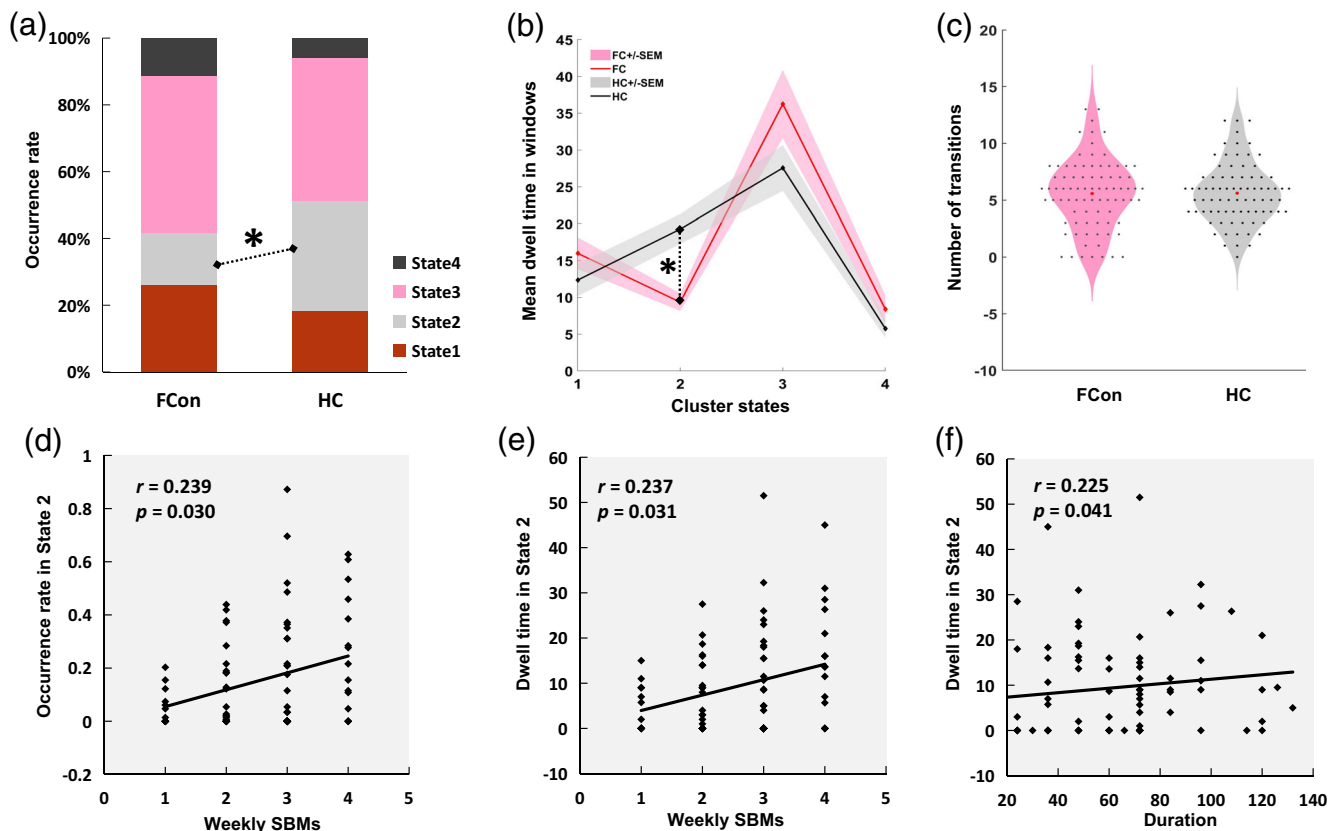

FIGURE 4   The temporal properties of the dFC states in FCon patients and HS. (a,b) The between-group comparisons of occurrence rate and mean dwell time in each state. The asterisk represents the significant difference under the threshold of p_{FDR} < .05. (c) The between-group comparison of the number of transitions. The black dot indicates each subject, and the red dot indicates the mean of transitions number. (d–f) Scatterplots of the correlation between the clinical symptoms and temporal properties in State 2. FCon, functional constipation; HS, healthy subjects; weekly SBMs, weekly spontaneous bowel movements; *SEM*, standard error of mean

3.4 | aINS–cortical coupling patterns in State 2

Given the significant alterations of temporal properties of State 2 in FCon patients, as well as the critical role of aINS in the central patho-logical alterations of FCon, we conducted the between-group compar-isons of the connectivities between the aINS (IC 17) and other 59 ICs in State 2, so as to investigate the differences of dynamic functional coupling patterns between FCon patients and HS. As shown in Figure 3, 53 of the 83 FCon patients and 64 of the 80 HS expressed State 2, so the between-group comparisons and correlation analyses were performed based on these participants.

The results of between-group comparisons demonstrated that there were eight aINS-related connections shown significant differences between FCon patients and HS. Specifically, FCon patients had stronger functional connectivity of aINS-anterior cingulate cortex (ACC, IC39), aINS-posterior cingulate cortex and medial orbitofrontal gyrus (IC49), aINS-right angular gyrus (IC68), aINS-CB crus II (IC70) connections, and weaker functional connectivity of aINS-thalamus (IC73), aINS-superior frontal gyrus (IC44), aINS-lingual gyrus (IC24), aINS-superior occipital gyrus (IC42) connections than HS in State 2 ($p_{FDR} < .05$), which are dis-played with the black rectangular boxes in the matrix in Figure 5. Results of correlation analyses indicated that the aINS-ACC connection, as well as aINS-CB crus II connection were positively correlated with the PAC-SYM scores in FCon patients ($r = .400$, $p = .003$, $p_{FDR} < .05$; $r = .425$, $p = .002$, $p_{FDR} < .05$) (Figure 5).

After regressing out the influences of age, gender, mean FD, SAS score, and SDS score, the between-group differences of the aINS-IC68, aINS-IC73, and aINS-IC42 connections were no longer signifi-cant, while the differences of aINS-Caudate (IC66) and aINS-middle occipital gyrus (IC72) connections became significant ($p_{FDR} < .05$). Similarly, the correlations of aINS-ACC, aINS-CB crus II connections, and PAC-SYM scores maintained significant even controlling these covariates ($r = .379$, $p = .008$, $p_{FDR} < .05$; $r = .382$, $p = .007$, $p_{FDR} < .05$) (Supplementary information 4c,d).

Additionally, we further compared the connectivity patterns of these eight aINS-related connections in other three states, finding that the aINS-IC73 connection in State 1 and aINS-IC49 connection in State 3 manifested significant between-group differences. How-ever, no significant correlation between these two connections and clinical symptoms was detected (Supplementary information 6).

3.5 | Dynamic graph-theoretic analysis

In addition to the dynamics of global topological metrics, we were also interested in the nodal topological metrics of the aINS. Supplementary information 7 illustrates the dynamic changes of these topological metrics across windows in all participants. As shown in Figure 6, FCon patients had higher SampEn at E_{nodal} of aINS (FCon patients: 0.527 ± 0.099, HS: 0.483 ± 0.116, $p = .01$, $p_{FDR} < .05$) than HS. However,
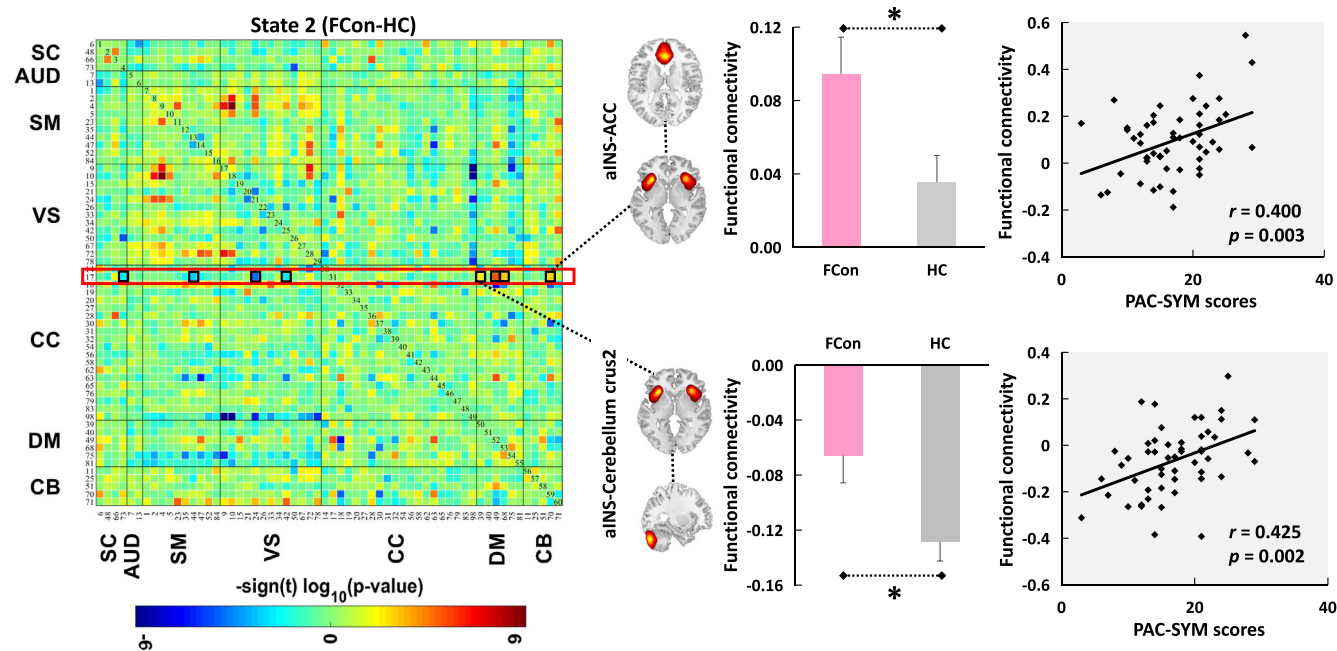

FIGURE 5 Aberrant aINS–cortical coupling patterns in State 2 and their associations with constipation symptoms. There were eight aINS related connections, including aINS-ACC and aINS-cerebellum crus II manifested a significant difference between FCon patients and HS (shown with the black rectangular boxes in the matrix). The asterisk represents the significant difference under the threshold of $p_{FDR} < 0.05$. The aberrant coupling patterns of aINS-ACC and aINS-cerebellum crus II were positively correlated with PAC-SYM scores in FCon patients. ACC, anterior cingulate cortex; aINS, anterior insula; AUD, auditory network; CB, cerebellum network; CC, cognitive control network; DM, default mode network; FCon, functional constipation; HS, healthy subjects; PAC-SYM, Patient Assessment of Constipation Symptom Questionnaire; SC, subcortical network; SM, sensorimotor network; VS, visual network
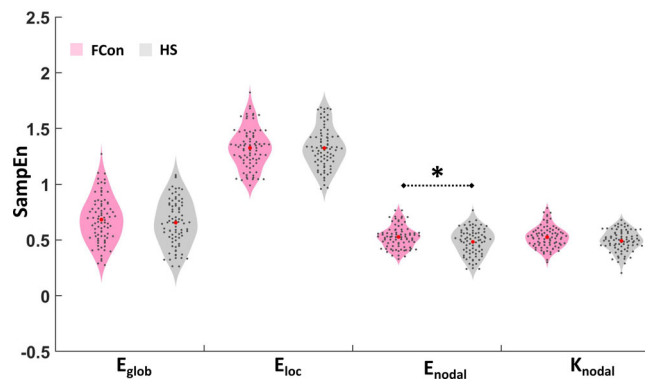
FIGURE 6 Between-group comparisons of SampEn of the global and nodal topological metrics. A black dot indicates a subject, and the red dot indicates the mean of SampEn. The asterisk represents the significant difference under the threshold of $p_{FDR} < .05$. E_{glob}, global efficiency; E_{loc}, local efficiency; E_{nodal}, nodal efficiency; FCon, functional constipation; HS, healthy subjects; K_{nodal}, nodal degree; SampEn, sample entropy

there was no significant difference was found in SampEn at E_{glob} (FCon patients: 0.683 ± 0.209, HS: 0.655 ± 0.208, $p = .401$), E_{loc} (FCon patients: 1.326 ± 0.181, HS: 1.324 ± 0.183, $p = .961$) and K_{nodal} of aINS (FCon patients: 0.525 ± 0.098, HS: 0.492 ± 0.095, $p = .03$, $p_{FDR} > .05$). Unsurprisingly, the above findings were maintained the same after controlling influences of the age, gender, mean FD, SAS score, and SDS score.

Furthermore, we performed the exploratory analysis by comparing the SampEn of E_{nodal} and K_{nodal} of the other 59 nodes. The results indicated that FCon patients had higher SampEn at E_{nodal} of the inferior temporal gyrus (IC62) and higher SampEn at K_{nodal} of the medial thalamus (IC48), the caudate (IC66), and the inferior orbitofrontal gyrus (IC56) than HS ($p_{uncorrected} < .05$). However, these between-group differences were not significant under the FDR corrected threshold. The results of the exploratory analysis are shown in Supplementary information 8.

4 | DISCUSSION

This was the first work to investigate the dFC patterns of FGIDs patients. The findings supported the hypothesis that FCon patients had symptom-related disrupted dynamic connectivity patterns and atypical dynamic topological organizations in the intrinsic functional brain networks.

4.1 | Absence of DM-CC co-activation state in FCon patients

A growing number of studies have indicated that both rats (Matsui, Murakami, & Ohki, 2019; Thompson, Pan, Magnuson, Jaeger, & Keilholz, 2014) and human beings (Calhoun et al., 2014; Mäki-

Marttunen & Espeseth, 2021) manifested periodic recurrence of functional brain connectivity over several minutes of resting-state scanning, which were attributed to the direct product of underlying neural electrical activity (Matsui et al., 2019; Thompson et al., 2013). To describe the periodic fluctuations of spatio-temporal connectivity patterns in the human brain, Allen et al. (2014) introduced the k-means clustering-based dFC analysis, which has been regarded as a promising approach for investigating the time-variation of the brain's intrinsic organizations at resting state. The description of the time-varying characteristics of the brain, that is, the temporal properties of the reoccurring functional connectivity states, is accepted as a sensitive indicator of the integration and separation properties of brain function, as well as a novel biomarker for several neurological diseases (Schumacher et al., 2019; Shine et al., 2019; Sun, Collinson, Suckling, & Sim, 2019) and pain disorders (Mäki-Marttunen & Espeseth, 2021; Tu et al., 2019).

In the present study, we identified four reoccurring functional connectivity states and found that FCon patients had an abnormal proportion of time spent in State 2. Besides, these aberrant temporal properties of State 2 were associated with the severity of constipation symptoms in FCon patients. As described above, the most noticeable features that distinguished State 2 from the other three states were the tight and complex connections between CC and DM. The decrease of the fractional windows in State 2 indicated the absence of complex co-activation between CC and DM in FCon patients. These absent co-activation patterns could specifically characterize the pathophysiological features of the diseases. Several studies have demonstrated that FCon patients had atypical static functional connectivity between regions in the CC and DM (Icenhour et al., 2017; Jin et al., 2019; Mayer et al., 2019). The present study further demonstrated from the temporal dimension that FCon patients manifested the absence of functional connectivity states with the complex DM-CC connection, which provided the new insight for explaining the altered functional connectivity strength between CC and DM in FCon patients. Given that CC and DM are both highly involved in coordinating information, especially the endogenous information of the human body (Cole, Pathak, & Schneider, 2010), this finding may suggest that FCon patients have impairments in endogenous task processing due to the absent communication between CC and DM.

4.2 | Aberrance of aINS–cortical coupling patterns in FCon patients

The present work demonstrated that FCon patients manifested symptoms-related alterations in aINS-ACC and aINS-CB crus II connectivity in State 2, but not in the other three states. This finding suggested that the connectivity patterns which were characterized at the state with aberrant temporal properties could better reveal the pathophysiology of the disease than other states. Therefore, the dFC might be more appropriate for investigating the characteristics of brain networks in disease than static analysis because of its ability to filter out the nonrelevant stable connectivity states.

The aINS is the core node of viscerosensory reception and processing. The ACC is the hub of multisensory information integration. Together, these two regions participate in the perception of gut feeling, maintaining gastrointestinal homeostasis, and recall of interoceptive memories (Mayer, 2011; Mayer et al., 2019). Several studies have demonstrated that patients with FGIDs (Bednarska et al., 2019; Zeng et al., 2011), including FCon (Jin et al., 2019; Zhu et al., 2016) manifested the symptoms-related abnormal activity patterns in the aINS and ACC. This study observed a significant correlation between the symptom severity and the abnormally increased aINS-ACC connectivity at FCon patients, suggesting that the aberrant co-activation between aINS and ACC might be a critical central pathological feature of FCon patients. The aINS and ACC are the principal components of the salience network, which responds to the experience and expectation of interoceptive or exteroceptive stimulus and engages in the coordination of the appropriate attentional, behavioral, affective, and visceral responses to such stimuli (Mayer et al., 2019). Therefore, the abnormal functional connectivity between aINS and ACC may suggest that FCon patients had reduced perception and responsiveness to gut stimuli. Moreover, the aINS and ACC are the key nodes of the central autonomic network, which is responsible for regulating autonomic function and thereby modulating visceral activity (Roy & Green, 2019). The incoordination between aINS and ACC leads to the disorders of sympathetic and sacral parasympathetic activities (Paulus & Stein, 2006) and disturbs the homeostasis of the gut through modulating multiple target cells that affect motility and secretion of the distal colon (Tong, Ridolfi, Kosinski, Ludwig, & Takahashi, 2010), which in turn causes the symptoms of constipation.

The CB is traditionally thought to be primarily responsible for the somatomotor function, while the recent study demonstrated that the CB might also be implicated in the perception and regulation of visceral sensations (Diedrichsen, King, Hernandez-Castillo, Sereno, & Ivry, 2019). When exposing to the rectal balloon distension, patients with irritable bowel syndrome manifested stronger activation in the aINS and CB crus II than HS, and the intensity of the activation gradually enhanced as the volume of the rectal balloon increasing (Guleria et al., 2017; Wang, Zhang, Zhang, Huang, & Song, 2017). These results suggested that the aINS and CB crus II directly participated in the perception of abnormal gut sensations. Interestingly, a recent animal experiment found that Purkinje cells in the CB crus I and II engaged in the control and coordination of voluntary and autonomic rhythmic behaviors (Romano et al., 2020). As we know, bowel movement depends on the rhythmic peristalsis of the colon, which is mainly controlled by the central autonomic network. Therefore, we speculated that the disrupted functional connectivity between CB crus II and aINS might explain the dual impairments in colonic sensory perception and autonomic rhythmic peristalsis in FCon patients, which was highly consistent with the most widely recognized pathogenic mechanism of FCon, the disturbance of colonic SM (Bharucha & Lacy, 2020).

As Rome Working Team reported (Van Oudenhove et al., 2016), the FGIDs generally resulted from complex interactions among biological, psychological, and social factors. In addition to the disturbance of colonic SM, the attack of FCon is also tightly associated with negative emotions, insufficient perception of constipation, and psychosocial disorders (Hu et al., 2020). Considering the critical role of aINS and ACC in processing cognitive and emotional tasks, as well as the extensive anatomical connections and functional coupling of the CB crus II with aINS and DM (Buckner, Krienen, Castellanos, Diaz, & Yeo, 2011; Kelly & Strick, 2003), we speculated that the similar alterations of functional connectivity patterns between aINS and multiple DM regions as well as CB crus II might suggest the abnormalities in emotion regulation and CC in FCon patients.

4.3 | Atypical dynamics of regional network topological properties in FCon patients

The network topological properties incarnate the efficiency of information transmission in brain networks. This study introduced SampEn, a metric reflecting the disorderliness of temporal signal, for the first time to measure the dynamics of network topological organizations at the time scale of seconds. The finding manifested that the SampEn of the aINS efficiency rather than the global efficiency was significantly higher in FCon patients than in HS. It suggested that FCon patients manifested disorderliness and instability of regional parallel information transmission that had not yet infiltrated the whole brain. Similarly, in a recent static graph-theoretic analysis (Liu et al., 2021), researchers did not find the alterations in E_{loc} and E_{glob} but observed aberrant nodal topological properties of the aINS and thalamus in FCon patients. These results together indicated a regional instead of global abnormality in information transmission in FCon patients and reiterated the importance of the aINS activity patterns in the central pathophysiology model of FCon.

Several limitations should be concerned in this study. First, this study applied the resting-state design. The current findings reflected the spontaneous transitions of functional connectivity in FCon patients only. In the future, the dFC analysis based on task fMRI dataset is worthy to be conducted, so as to provide deeper insights into the dynamic alterations of the brain co-activation patterns under certain stimuli (such as a sensory or emotional task). Second, due to the gender differences in FCon prevalence and the gender imbalance of the recruiting sites, females were much more numerous than males in this study. As a result, the post hoc comparison between male and female patients could not be conducted. Given that previous studies have reported the gender-related differences in static functional connectivity in FCon (Jin et al., 2019) and many other FGIDs (Houghton et al., 2016), whether there are significant gender differences in dFC patterns in FCon patients warrants further study. Third, although the enrolled patients did not take any medication in the past 15 days, the influence of former medication use on the brain function could still not be eliminated entirely. Fourthly, satisfactory temporal resolution and sufficient length of data acquisition are important for the reliability of dFC analysis. Although several studies (Mäki-Marttunen & Espeseth, 2021; Tu et al., 2019) have reliably shown that dynamics of brain activity could be successfully sampled with the same parameters as our study (TR = 2 s, time points = 180), we believed that a higher

temporal-resolution MRI and a long time of data acquisition to sample more dense time series would be meaningful for evaluating dynamic properties of the diseases.

5 | CONCLUSION

In summary, this study demonstrated the disruptions of dFC patterns in FCon patients from the respects of the absence of DM-CC connection states, aberrance of aINS–cortical coupling patterns as well as atypical dynamics of regional topological organizations. The current findings provided dynamic perspectives for understanding the brain connectome of FCon and laid the foundation for the potential treatment of FCon based on brain connectomics.

CONFLICT OF INTERESTS

The authors declare no conflict of interests.

AUTHOR CONTRIBUTIONS

Tao Yin: Conceptualization, methodology, software, writing-original draft, investigation. **Zhaoxuan He**: Data curation, project administration, supervision, writing-review and editing. **Peihong Ma**: Investigation, validation, methodology. **Ruirui Sun**: Validation, supervision. **Kunnan Xie**: Investigation, formal analysis. **Tianyu Liu**: Investigation. **Li Chen**: Investigation. **Jingwen Chen**: Investigation. **Likai Hou**: Investigation. **Yuke Teng**: Investigation. **Yuyi Guo**: Investigation. **Zilei Tian**: Investigation, software. **Jing Xiong**: Formal analysis. **Fumin Wang**: Investigation. **Shenghong Li**: Resources. **Sha Yang**: Conceptualization, project administration, resources. **Fang Zeng**: Conceptualization, funding acquisition, writing-review and editing.

DATA AVAILABILITY STATEMENT

Data in this manuscript is a part of a longitudinal study that will generate more than one manuscript. The data will be available once these manuscripts are completed. Reasonable requests for data can be sent to the corresponding author (F. Z.).

ETHICS APPROVAL AND PATIENT CONSENT STATEMENT

This study was approved by the Institutional Review Boards and Ethics Committees of the Hospital of Chengdu University of Traditional Chinese Medicine (Approved number: 2018KL-022). Informed consent was obtained from each participant.

ORCID

Tao Yin https://orcid.org/0000-0002-9429-7153

REFERENCES

Allen, E. A., Damaraju, E., Plis, S. M., Erhardt, E. B., Eichele, T., & Calhoun, V. D. (2014). Tracking whole-brain connectivity dynamics in the resting state. *Cerebral Cortex*, *24*, 663–676.

Arco, S., Saldaña, E., Serra-Prat, M., Palomera, E., Ribas, Y., Font, S., ... Mundet, L. (2021). Functional constipation in older adults: Prevalence, clinical symptoms and subtypes, association with frailty, and impact on quality of life. *Gerontology*, 1–10. https://doi.org/10.1159/000517212.

Barberio, B., Judge, C., Savarino, E. V., & Ford, A. C. (2021). Global prevalence of functional constipation according to the Rome criteria: A systematic review and meta-analysis. *The Lancet Gastroenterology and Hepatology*, *6*, 638–648.

Bednarska, O., Icenhour, A., Tapper, S., Witt, S. T., Tisell, A., Lundberg, P., ... Walter, S. (2019). Reduced excitatory neurotransmitter levels in anterior insulae are associated with abdominal pain in irritable bowel syndrome. *Pain*, *160*, 2004–2012.

Behzadi, Y., Restom, K., Liau, J., & Liu, T. T. (2007). A component based noise correction method (CompCor) for BOLD and perfusion based fMRI. *NeuroImage*, *37*, 90–101.

Bell, A. J., & Sejnowski, T. J. (1995). An information-maximization approach to blind separation and blind deconvolution. *Neural Computation*, *7*, 1129–1159.

Bharucha, A. E., & Lacy, B. E. (2020). Mechanisms, evaluation, and management of chronic constipation. *Gastroenterology*, *158*, 1232–1249.e3.

Biswal, B., Yetkin, F. Z., Haughton, V. M., & Hyde, J. S. (1995). Functional connectivity in the motor cortex of resting human brain using echo-planar MRI. *Magnetic Resonance in Medicine*, *34*, 537–541.

Black, C. J., Drossman, D. A., Talley, N. J., Ruddy, J., & Ford, A. C. (2020). Functional gastrointestinal disorders: Advances in understanding and management. *Lancet*, *396*, 1664–1674.

Buckner, R. L., Krienen, F. M., Castellanos, A., Diaz, J. C., & Yeo, B. T. (2011). The organization of the human cerebellum estimated by intrinsic functional connectivity. *Journal of Neurophysiology*, *106*, 2322–2345.

Calhoun, V. D., Adali, T., Pearlson, G. D., & Pekar, J. J. (2001). A method for making group inferences from functional MRI data using independent component analysis. *Human Brain Mapping*, *14*, 140–151.

Calhoun, V. D., Miller, R., Pearlson, G., & Adalı, T. (2014). The chronnectome: Time-varying connectivity networks as the next frontier in fMRI data discovery. *Neuron*, *84*, 262–274.

Chang, C., & Glover, G. H. (2010). Time-frequency dynamics of resting-state brain connectivity measured with fMRI. *NeuroImage*, *50*, 81–98.

Ciric, R., Wolf, D. H., Power, J. D., Roalf, D. R., Baum, G. L., Ruparel, K., ... Satterthwaite, T. D. (2017). Benchmarking of participant-level confound regression strategies for the control of motion artifact in studies of functional connectivity. *NeuroImage*, *154*, 174–187.

Cole, M. W., Pathak, S., & Schneider, W. (2010). Identifying the brain's most globally connected regions. *NeuroImage*, *49*, 3132–3148.

Craig, A. D. (2009). How do you feel—now? The anterior insula and human awareness. *Nature Reviews Neuroscience*, *10*, 59–70.

Diedrichsen, J., King, M., Hernandez-Castillo, C., Sereno, M., & Ivry, R. B. (2019). Universal transform or multiple functionality? Understanding the contribution of the human cerebellum across task domains. *Neuron*, *102*, 918–928.

Díez-Cirarda, M., Strafella, A. P., Kim, J., Peña, J., Ojeda, N., Cabrera-Zubizarreta, A., & Ibarretxe-Bilbao, N. (2018). Dynamic functional connectivity in Parkinson's disease patients with mild cognitive impairment and normal cognition. *NeuroImage: Clinical*, *17*, 847–855.

Drossman, D. A., & Hasler, W. L. (2016). Rome IV-functional GI disorders: Disorders of gut-brain interaction. *Gastroenterology*, *150*, 1257–1261.

Duan, S., Liu, L., Li, G., Wang, J., Hu, Y., Zhang, W., ... Cui, G. (2021). Altered functional connectivity within and between salience and sensorimotor networks in patients with functional constipation. *Frontiers in Neuroscience*, *15*, 628880.

Easson, A. K., & McIntosh, A. R. (2019). BOLD signal variability and complexity in children and adolescents with and without autism spectrum disorder. *Developmental Cognitive Neuroscience, 36*, 100630.

Fiorenzato, E., Strafella, A. P., Kim, J., Schifano, R., Weis, L., Antonini, A., & Biundo, R. (2019). Dynamic functional connectivity changes associated with dementia in Parkinson's disease. *Brain, 142*, 2860–2872.

Friedman, J., Hastie, T., & Tibshirani, R. (2008). Sparse inverse covariance estimation with the graphical lasso. *Biostatistics, 9*, 432–441.

Guleria, A., Karyampudi, A., Singh, R., Khetrapal, C. L., Verma, A., Ghoshal, U. C., & Kumar, D. (2017). Mapping of brain activations to rectal balloon distension stimuli in male patients with irritable bowel syndrome using functional magnetic resonance imaging. *Journal of Neurogastroenterology and Motility, 23*, 415–427.

Himberg, J., Hyvärinen, A., & Esposito, F. (2004). Validating the independent components of neuroimaging time series via clustering and visualization. *NeuroImage, 22*, 1214–1222.

Houghton, L. A., Heitkemper, M., Crowell, M., Emmanuel, A., Halpert, A., McRoberts, J. A., & Toner, B. (2016). Age, gender and women's health and the patient. *Gastroenterology, 150*, 1332–1343.e4.

Hu, C., Liu, L., Liu, L., Zhang, J., Hu, Y., Zhang, W., ... Zhang, Y. (2020). Cortical morphometry alterations in brain regions involved in emotional, motor-control and self-referential processing in patients with functional constipation. *Brain Imaging and Behavior, 14*(5), 1899–1907.

Hutchison, R. M., Womelsdorf, T., Allen, E. A., Bandettini, P. A., Calhoun, V. D., Corbetta, M., ... Chang, C. (2013). Dynamic functional connectivity: Promise, issues, and interpretations. *NeuroImage, 80*, 360–378.

Icenhour, A., Witt, S. T., Elsenbruch, S., Lowén, M., Engström, M., Tillisch, K., ... Walter, S. (2017). Brain functional connectivity is associated with visceral sensitivity in women with irritable bowel syndrome. *NeuroImage: Clinical, 15*, 449–457.

Jin, Q., Duan, S., Li, G., Sun, L., Hu, Y., Hu, C., ... Zhang, Y. (2019). Sex-related differences in resting-state brain activity and connectivity in the orbital frontal cortex and insula in patients with functional constipation. *Neurogastroenterology and Motility, 31*, e13566.

Kelly, R. M., & Strick, P. L. (2003). Cerebellar loops with motor cortex and prefrontal cortex of a nonhuman primate. *The Journal of Neuroscience, 23*, 8432–8444.

Kim, J., Criaud, M., Cho, S. S., Díez-Cirarda, M., Mihaescu, A., Coakeley, S., ... Strafella, A. P. (2017). Abnormal intrinsic brain functional network dynamics in Parkinson's disease. *Brain, 140*, 2955–2967.

Lacy, B. E., Mearin, F., Chang, L., Chey, W. D., Lembo, A. J., Simren, M., & Spiller, R. (2016). Bowel disorders. *Gastroenterology, 150*, 1393–1407.e5.

Li, G., Zhang, W., Hu, Y., Wang, J., Li, J., Jia, Z., ... Nie, Y. (2021). Distinct basal brain functional activity and connectivity in the emotional-arousal network and thalamus in patients with functional constipation associated with anxiety and/or depressive disorders. *Psychosomatic Medicine, 83*, 707–714.

Li, J., Duan, X., Cui, Q., Chen, H., & Liao, W. (2019). More than just statics: Temporal dynamics of intrinsic brain activity predicts the suicidal ideation in depressed patients. *Psychological Medicine, 49*, 852–860.

Liu, L., Hu, C., Hu, Y., Zhang, W., Zhang, Z., Ding, Y., ... Zhang, Y. (2021). Abnormalities in the thalamo-cortical network in patients with functional constipation. *Brain Imaging and Behavior, 15*, 630–642.

Luppi, A. I., Craig, M. M., Pappas, I., Finoia, P., Williams, G. B., Allanson, J., ... Stamatakis, E. A. (2019). Consciousness-specific dynamic interactions of brain integration and functional diversity. *Nature Communications, 10*, 4616.

Mäki-Marttunen, V., & Espeseth, T. (2021). Uncovering the locus coeruleus: Comparison of localization methods for functional analysis. *NeuroImage, 224*, 117409.

Matsui, T., Murakami, T., & Ohki, K. (2019). Neuronal origin of the temporal dynamics of spontaneous BOLD activity correlation. *Cerebral Cortex, 29*, 1496–1508.

Mayer, E. A. (2011). Gut feelings: The emerging biology of gut-brain communication. *Nature Reviews. Neuroscience, 12*, 453–466.

Mayer, E. A., Labus, J., Aziz, Q., Tracey, I., Kilpatrick, L., Elsenbruch, S., ... Borsook, D. (2019). Role of brain imaging in disorders of brain-gut interaction: A Rome working team report. *Gut, 68*, 1701–1715.

Nag, A., Martin, S. A., Mladsi, D., Olayinka-Amao, O., Purser, M., & Vekaria, R. M. (2020). The humanistic and economic burden of chronic idiopathic constipation in the USA: A systematic literature review. *Clinical and Experimental Gastroenterology, 13*, 255–265.

Nan, J., Zhang, L., Chen, Q., Zong, N., Zhang, P., Ji, X., ... Zhang, M. (2018). White matter microstructural similarity and diversity of functional constipation and constipation-predominant irritable bowel syndrome. *Journal of Neurogastroenterology and Motility, 24*, 107–118.

Nezafati, M., Temmar, H., & Keilholz, S. D. (2020). Functional MRI signal complexity analysis using sample entropy. *Frontiers in Neuroscience, 14*, 700.

Osadchiy, V., Mayer, E. A., Gao, K., Labus, J. S., Naliboff, B., Tillisch, K., ... Gupta, A. (2020). Analysis of brain networks and fecal metabolites reveals brain-gut alterations in premenopausal females with irritable bowel syndrome. *Translational Psychiatry, 10*, 367.

Pascual-Marqui, R. D., Michel, C. M., & Lehmann, D. (1995). Segmentation of brain electrical activity into microstates: Model estimation and validation. *IEEE Transactions on Bio-Medical Engineering, 42*, 658–665.

Paulus, M. P., & Stein, M. B. (2006). An insular view of anxiety. *Biological Psychiatry, 60*, 383–387.

Peihong, M., Tao, Y., Zhaoxuan, H., Sha, Y., Li, C., Kunnan, X., ... Fang, Z. (2021). Alterations of white matter network properties in patients with functional constipation. *Frontiers in Neurology, 12*, 627130.

Power, J. D., Barnes, K. A., Snyder, A. Z., Schlaggar, B. L., & Petersen, S. E. (2012). Spurious but systematic correlations in functional connectivity MRI networks arise from subject motion. *NeuroImage, 59*, 2142–2154.

Preti, M. G., Bolton, T. A., & Van De Ville, D. (2017). The dynamic functional connectome: State-of-the-art and perspectives. *NeuroImage, 160*, 41–54.

Richman, J. S., & Moorman, J. R. (2000). Physiological time-series analysis using approximate entropy and sample entropy. *American Journal of Physiology. Heart and Circulatory Physiology, 278*, H2039–H2049.

Romano, V., Reddington, A. L., Cazzanelli, S., Mazza, R., Ma, Y., Strydis, C., ... De Zeeuw, C. I. (2020). Functional convergence of autonomic and sensorimotor processing in the lateral cerebellum. *Cell Reports, 32*, 107867.

Roy, H. A., & Green, A. L. (2019). The central autonomic network and regulation of bladder function. *Frontiers in Neuroscience, 13*, 535.

Rubinov, M., & Sporns, O. (2010). Complex network measures of brain connectivity: Uses and interpretations. *NeuroImage, 52*, 1059–1069.

Rubio, A., Van Oudenhove, L., Pellissier, S., Ly, H. G., Dupont, P., Lafaye de Micheaux, H., ... Bonaz, B. (2015). Uncertainty in anticipation of uncomfortable rectal distension is modulated by the autonomic nervous system—A fMRI study in healthy volunteers. *NeuroImage, 107*, 10–22.

Schumacher, J., Peraza, L. R., Firbank, M., Thomas, A. J., Kaiser, M., Gallagher, P., ... Taylor, J. P. (2019). Dysfunctional brain dynamics and their origin in Lewy body dementia. *Brain, 142*, 1767–1782.

Serra, J., Pohl, D., Azpiroz, F., Chiarioni, G., Ducrotté, P., Gourcerol, G., ... Whorwell, P. (2020). European society of neurogastroenterology and motility guidelines on functional constipation in adults. *Neurogastroenterology and Motility, 32*, e13762.

Shafiei, G., Zeighami, Y., Clark, C. A., Coull, J. T., Nagano-Saito, A., Leyton, M., ... Mišic, B. (2019). Dopamine signaling modulates the stability and integration of intrinsic brain networks. *Cerebral Cortex, 29*, 397–409.

Shan, Z. Y., Finegan, K., Bhuta, S., Ireland, T., Staines, D. R., Marshall-Gradisnik, S. M., & Barnden, L. R. (2018). Brain function characteristics of chronic fatigue syndrome: A task fMRI study. *NeuroImage: Clinical, 19*, 279–286.

Shine, J. M., Bell, P. T., Matar, E., Poldrack, R. A., Lewis, S. J. G., Halliday, G. M., & O'Callaghan, C. (2019). Dopamine depletion alters macroscopic network dynamics in Parkinson's disease. *Brain*, *142*, 1024–1034.

Smith, S. M., Miller, K. L., Salimi-Khorshidi, G., Webster, M., Beckmann, C. F., Nichols, T. E., … Woolrich, M. W. (2011). Network modelling methods for FMRI. *NeuroImage*, *54*, 875–891.

Sun, Y., Collinson, S. L., Suckling, J., & Sim, K. (2019). Dynamic reorganization of functional connectivity reveals abnormal temporal efficiency in schizophrenia. *Schizophrenia Bulletin*, *45*, 659–669.

Thompson, G. J., Merritt, M. D., Pan, W. J., Magnuson, M. E., Grooms, J. K., Jaeger, D., & Keilholz, S. D. (2013). Neural correlates of time-varying functional connectivity in the rat. *NeuroImage*, *83*, 826–836.

Thompson, G. J., Pan, W. J., Magnuson, M. E., Jaeger, D., & Keilholz, S. D. (2014). Quasi-periodic patterns (QPP): Large-scale dynamics in resting state fMRI that correlate with local infraslow electrical activity. *NeuroImage*, *84*, 1018–1031.

Tong, W. D., Ridolfi, T. J., Kosinski, L., Ludwig, K., & Takahashi, T. (2010). Effects of autonomic nerve stimulation on colorectal motility in rats. *Neurogastroenterology and Motility*, *22*, 688–693.

Tu, Y., Fu, Z., Zeng, F., Maleki, N., Lan, L., Li, Z., … Kong, J. (2019). Abnormal thalamocortical network dynamics in migraine. *Neurology*, *92*, e2706–e2716.

Van Dijk, K. R., Sabuncu, M. R., & Buckner, R. L. (2012). The influence of head motion on intrinsic functional connectivity MRI. *NeuroImage*, *59*, 431–438.

Van Oudenhove, L., Crowell, M. D., Drossman, D. A., Halpert, A. D., Keefer, L., Lackner, J. M., … Levy, R. L. (2016). Biopsychosocial aspects of functional gastrointestinal disorders. *Gastroenterology*, *150*(6), 1355–1367.

Vriesman, M. H., Koppen, I. J. N., Camilleri, M., Di Lorenzo, C., & Benninga, M. A. (2020). Management of functional constipation in children and adults. *Nature Reviews. Gastroenterology & Hepatology*, *17*, 21–39.

Wang, D., Zhang, X., Zhang, X., Huang, Z., & Song, Y. (2017). Magnetic resonance imaging analysis of brain function in patients with irritable bowel syndrome. *BMC Gastroenterology*, *17*, 148.

Wang, J., Wang, X., Xia, M., Liao, X., Evans, A., & He, Y. (2015). GRETNA: A graph theoretical network analysis toolbox for imaging connectomics. *Frontiers in Human Neuroscience*, *9*, 386.

Wang, J. H., Zuo, X. N., Gohel, S., Milham, M. P., Biswal, B. B., & He, Y. (2011). Graph theoretical analysis of functional brain networks: Test-retest evaluation on short- and long-term resting-state functional MRI data. *PLoS One*, *6*, e21976.

Yan, C. G., Wang, X. D., Zuo, X. N., & Zang, Y. F. (2016). DPABI: Data processing & analysis for (resting-state) brain imaging. *Neuroinformatics*, *14*, 339–351.

Yin, T., He, Z., Ma, P., Hou, L., Chen, L., Xie, K., … Zeng, F. (2019). Effect and cerebral mechanism of acupuncture treatment for functional constipation: Study protocol for a randomized controlled clinical trial. *Trials*, *20*, 283.

Yu, M., Dai, Z., Tang, X., Wang, X., Zhang, X., Sha, W., … Zhang, Z. (2017). Convergence and divergence of brain network dysfunction in deficit and non-deficit schizophrenia. *Schizophrenia Bulletin*, *43*, 1315–1328.

Zeng, F., Qin, W., Liang, F., Liu, J., Tang, Y., Liu, X., … Tian, J. (2011). Abnormal resting brain activity in patients with functional dyspepsia is related to symptom severity. *Gastroenterology*, *141*, 499–506.

Zeng, F., Sun, R., He, Z., Chen, Y., Lei, D., Yin, T., … Kong, J. (2019). Altered functional connectivity of the amygdala and sex differences in functional dyspepsia. *Clinical and Translational Gastroenterology*, *10*, e00046.

Zhu, Q., Cai, W., Zheng, J., Li, G., Meng, Q., Liu, Q., … Nie, Y. (2016). Distinct resting-state brain activity in patients with functional constipation. *Neuroscience Letters*, *632*, 141–146.

Zhuang, X., Yang, Z., Mishra, V., Sreenivasan, K., Bernick, C., & Cordes, D. (2020). Single-scale time-dependent window-sizes in sliding-window dynamic functional connectivity analysis: A validation study. *NeuroImage*, *220*, 117111.

Zung, W. W. (1965). A self-rating depression scale. *Archives of General Psychiatry*, *12*, 63–70.

Zung, W. W. (1971). A rating instrument for anxiety disorders. *Psychosomatics*, *12*, 371–379.

SUPPORTING INFORMATION

Additional supporting information may be found in the online version of the article at the publisher's website.